JOURNAL OF MATERIALS SCIENCE 13 (1978) 2081–2091

Fracture phenomenology of a lithium-aluminium-silicate glass-ceramic

R. K. GOVILA, K. R. KINSMAN*, P. BEARDMORE
Research Staff, Ford Motor Company, Dearborn, Michigan 48121, USA

Crack propagation mechanisms in a lithium–aluminium-silicate glass-ceramic have been studied as a function of both initial flaw size and temperature. Using controlled surface cracks, the fracture stress at room temperature was found to conform to the Griffith flaw size dependence. Extrapolation suggests that processing flaws of the order of 6 to 8 μm are strength-controlling in the material investigated. Two mechanistic regimes were manifest in the temperature dependence of the fracture stress. Up to 900° C, catastrophic transgranular crack propagation occurred from emplaced cracks. At 1000° C and above, subcritical crack growth occurred intergranularly and the extent of slow crack growth prior to catastrophic failure increased with increasing temperature. The influence of loading rate on slow crack growth and fracture stress was explored at 950 and 1100° C. Generally, the extent of slow crack growth decreased with increased loading rate until at a sufficiently high rate, catastrophic fracture occurred directly with no slow crack extension. These results are discussed in terms of the role of plastic accommodation in the crack extension process, a phenomenon which seems mechanistically dependent upon remnant amorphous (uncrystallized) phase at grain boundaries.

1. Introduction

Lithium–aluminium-silicate (LAS) glass-ceramics are typically applied in situations that use to advantage their characteristic low thermal expansion. This, in combination with the practical utility of castability to nominally full density leads to the application of LAS in complex geometric parts. Similar to many other ceramic materials, LAS is generally regarded as a brittle material with little tolerance, from a structural viewpoint, for incipient flaws. The major purpose of the present work was to determine quantitatively the susceptibility of LAS to brittle fracture from inherent flaws and to evaluate the crack propagation mechanisms operative over a temperature range of practical use. By introducing controlled flaws into the material, an attempt has been made to measure certain of those parameters of strength that seem relevant to the mechanical response, namely, the effective fracture energy, γ, the factors which contribute to significant plasticity or viscous flow, and the effect of temperature and loading rate.

2. Experimental procedures and techniques

2.1. Sample preparation and testing

The particular material used for this study was a nominally fully dense lithium–aluminium-silicate of composition shown in Table I produced by Owen–Illinois under their code C-140. It is a crystallized glass ceramic comprised principally of the β-spodumene and β-eucryptite structures together with some impurities which aid in the material processing. In such glass-ceramics, generally, crystallization is nominally, though not entirely,

TABLE I Typical composition of lithium–aluminium silicate glass-ceramic (in wt %)

LiO_2	Al_2O_3	SiO_2	ZrO_2	TiO_2	ZnO	Sb_2O_3
3.9	18.0	73.0	1.7	1.7	1.3	0.4

*Now at Electric Power Research Institute, Palo Alto, California 94304, USA.

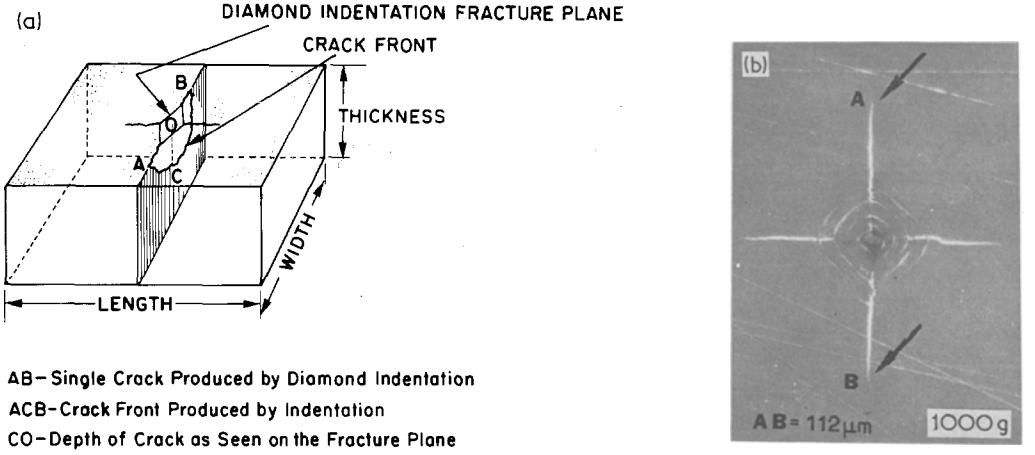

Figure 1 (a) Schematic representation of crack geometry in a specimen. (b) Typical example of a crack produced on the polished surface of LAS test specimen using a diamond pyramid indenter with 1000 g load. Picture taken in polarized light.

complete and residual glass tends to locate at crystalline interfaces either in pockets or as a thin viscous layer. Such small amounts of glassy phase are sure to escape detection in an otherwise crystalline matrix by all save the most sophisticated experimental techniques (e.g., lattice resolution via transmission electron microscopy). It is therefore normally accepted that some intergranular amorphous phase exists and the presence of this constituent must be considered in the material response. Consequently, to assess the possible contribution of residual glass to the phenomenon at hand, selected experiments were performed using material of identical composition but in the amorphous state.

Test specimens of dimensions 1 in. (~25 mm) long × 1/4 in. (~6 mm) wide × 1/8 in. (~3 mm) thick were machined from the block of LAS and all faces were ground to a 220 grit finish. One surface (the tension face in bending) was carefully hand ground and wet polished to a 6 μm diamond finish. After polishing, the specimens were heated for four hours in air at 200° C to remove any adsorbed water. Certain of the specimens were then precracked using the indentation technique as outlined briefly in Section 2.2, and tested in four-point bending in an Instron testing machine at a constant cross-head speed of 0.005 in. (~0.127 mm) min^{-1}. The outer and inner loading edges of the silicon carbide testing fixture were spaced 0.6 in. (~15 mm) and 0.2 in. (~5 mm) apart, respectively. High temperature (200 to 1200° C) bend tests were performed in air in a cylindrical muffle furnace (Centorr Associates). Fracture surfaces were examined by optical microscopy and scanning electron microscopy (SEM). For optical examination, a flash coating of aluminium was found to greatly enhance the reflectivity without any distortion of the fractographic features.

2.2. Controlled precracking of specimens

Indenting this material with a Vickers diamond pyramid indenter resulted in the introduction of surface cracks of reproducible geometry and size controlled by choice of indenter load. This technique has been used successfully both in single crystals of vanadium carbide [1] and in polycrystalline materials [2–6]. The resultant crack geometry and a typical example of a crack produced on the polished surface of a test specimen are shown in Figs. 1a and b, respectively. At indentation loads up to 1000 g, the crack fronts were approximately semi-circular but at higher loads (3000 to 5000 g) significant deviations from the semi-circular geometry occurred. All indentations were made at room temperature.

3. Results and discussion

3.1. Influence of crack size on fracture stress

The variation of fracture stress with controlled crack depth for LAS glass-ceramic specimens tested at room temperature is shown in Fig. 2. A reasonably good linear relationship is evident, consistent with the Griffith [7] criterion for brittle fracture:

$$\sigma_F \approx Y\left[\frac{E\gamma}{c}\right]^{1/2} \quad (1)$$

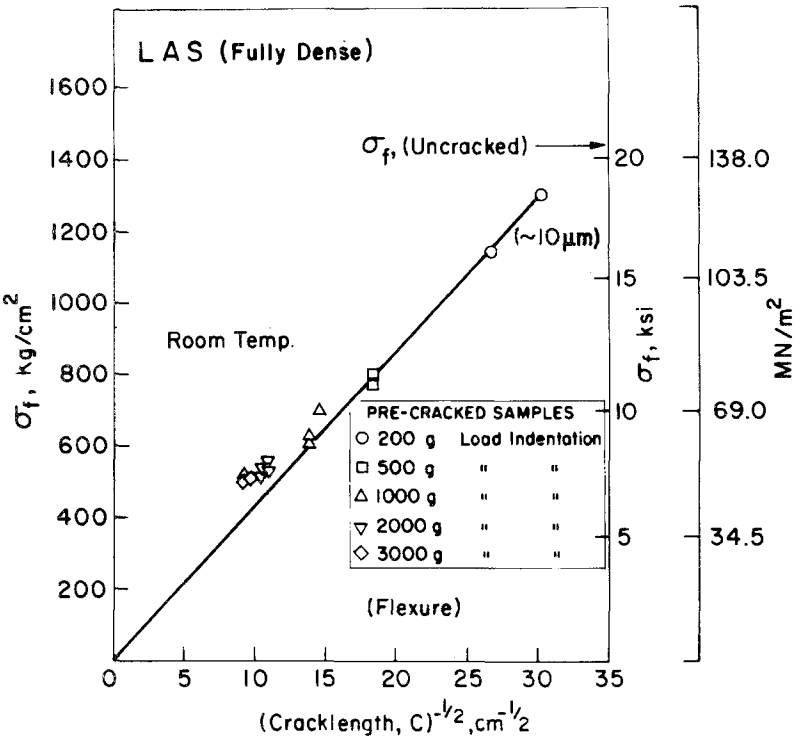

Figure 2 Variation of fracture stress as a function of (crack length or depth)$^{-1/2}$ at room temperature.

where σ_F is the fracture stress required to propagate a pre-existing crack of known dimensions, Y is a constant relating primarily to crack geometry and specimen dimensions, E is Young's modulus, c is the initial crack depth at which fracture initiated and γ is the fracture energy. For approximately semi-circular cracks, Y is taken as unity [1, 8]. Using a measured value of $E \approx 8.4 \times 10^{11}$ dyne cm^{-2} for LAS glass ceramic material at room temperature [9] and the slope of the curve shown in

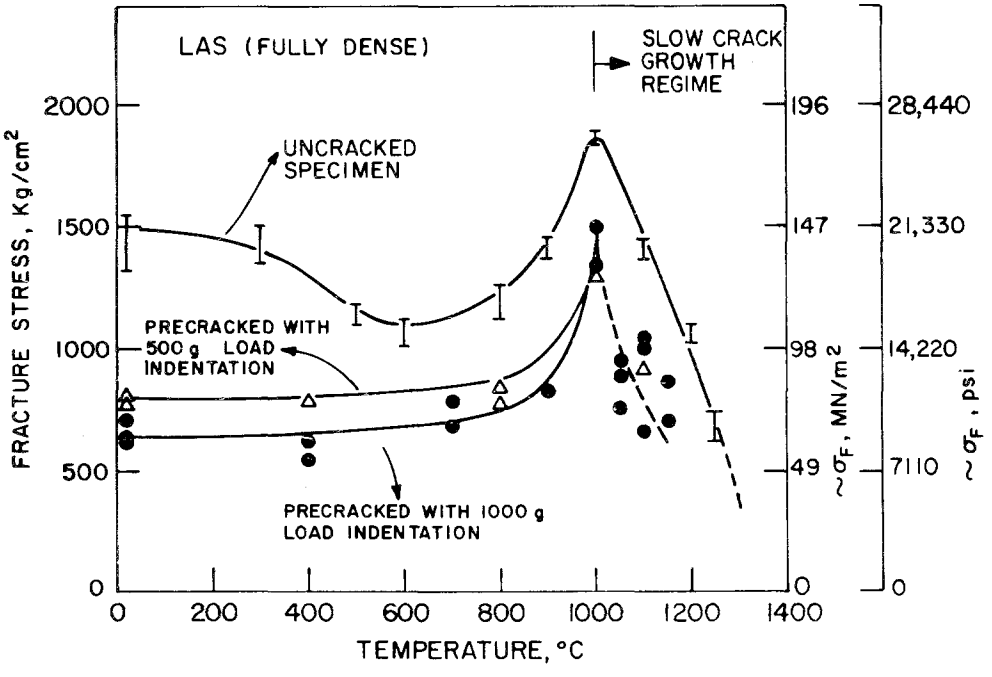

Figure 3 Effect of temperature on the fracture stress of uncracked, and precracked specimens. Specimens precracked with 500 g and 1000 g load indentation contained cracks of constant depth of approximately 32 μm and 52 μm, respectively.

Fig. 2, the computed value of fracture energy, γ, is $\sim 2150\,\mathrm{ergs\,cm^{-2}}$ at 20° C. This relatively low value of γ suggests that fracture occurs at this temperature in an essentially brittle manner involving little or no plasticity. It is imperative to note, however, that the above can be taken rigorously only as a demonstration of principle. A body of evidence is accumulating which suggests that crack opening residual stresses can accompany hardness indentation emplaced cracks in some materials [2, 3, 6, 10, 11]. While this feature apparently is not universal [12], the presence of such stress could significantly influence the absolute magnitude of the experimentally determined fracture energy. From a practical point of view, however, perhaps the most useful application of the data in Fig. 2 is as a means of estimating the inherent flaw size in the material. Extrapolation of the data in Fig. 2 to the fracture stress of uncracked samples implies that fracture initiating flaws of the order of 6 to 8 μm in size are present in the as-prepared LAS.

3.2. Effect of temperature on fracture behaviour

Three series of specimens were prepared for testing in the range 20 to 1200° C: a baseline series without any cracks, a second series precracked with 1000 g indentation load (cracks of about 52 μm depth) and a third series precracked with a 500 g indentation load (cracks of about 32 μm depth).

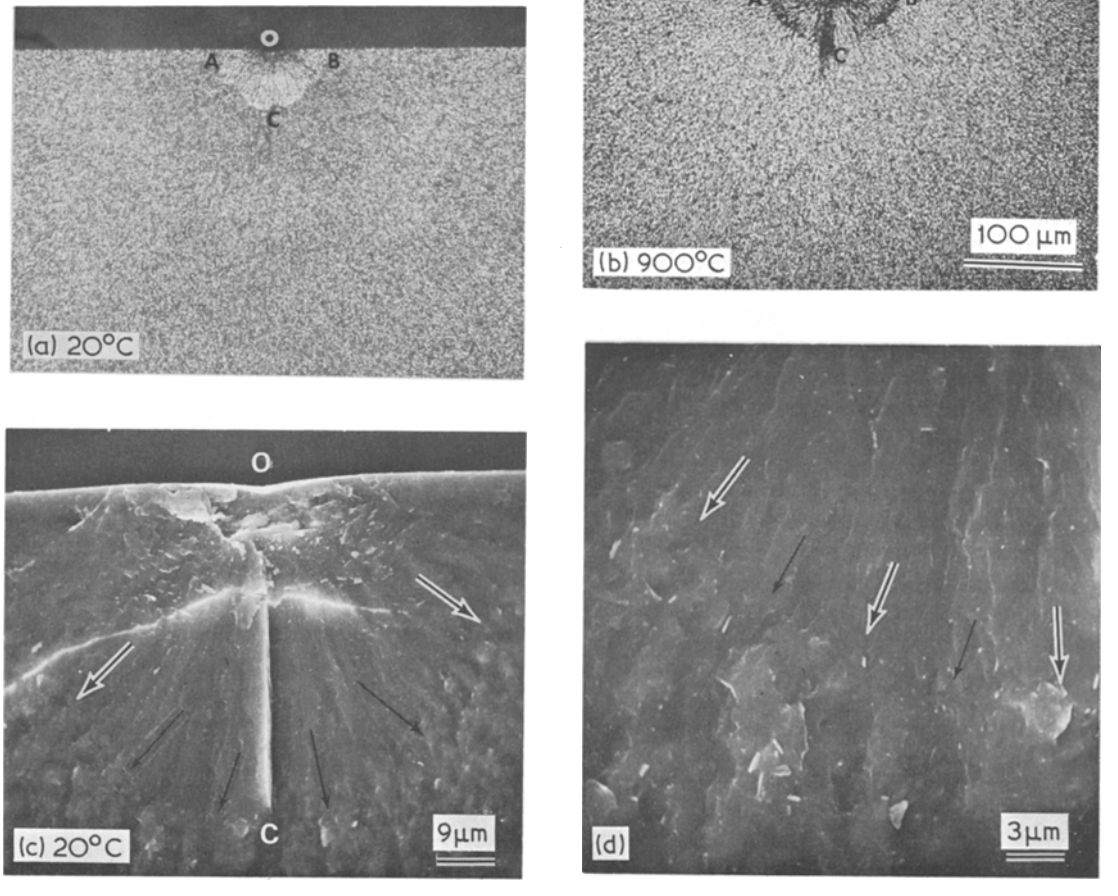

Figure 4 Typical cleavage fracture surfaces of LAS specimens precracked with 1000 g load indentation and subsequently tested in bending at 20 and 900° C. (a) and (b), optical fractographs at the marked temperatures. (c) and (d), typical fracture surface (same as in Fig. 4a) as viewed in SEM. (c) Detailed view of precracked region ACB. (d) Higher magnification view of precracked and repropagated regions along the crack front boundary ACB. Arrows identify the initial crack front boundary. Note that the mode of crack propagation in precracked and repropagated regions is similar and consists of transcrystalline cleavage.

The temperature dependence of the fracture stress is shown in Fig. 3, and it is evident that σ_F for precracked specimens remains essentially independent of temperature up to about 800° C. The constancy of σ_F in this temperature range implies that a single fracture mechanism predominates and that insignificant plastic deformation accompanied the fracture process.

Typical fracture topography of specimens tested at 20 and 900° C are shown in Fig. 4. An examination of the emplaced crack front boundary ACB was made at higher magnifications using the SEM, Figs. 4c and d, in order to ascertain any evidence of plastic flow. Fig. 4c shows a smooth precracked region (same specimen as seen in Fig. 4a) while Fig. 4d shows the boundary between the precracked and repropagated region without any signs of tearing along the crack front, thereby supporting the absence of plastic flow along the crack front ACB. Note that the mode of fracture in the precracked region and during subsequent crack propagation is similar, i.e., transcrystalline cleavage, Figs. 4c and d. Similar behaviour was observed in specimens up to 800° C while some roughness or tearing was visible on the fracture surface of specimens tested at 900° C. In all cases, within the regime up to 900° C, catastrophic failure occurred directly from the initial microcrack. The sudden and subsequent increase in σ_F at temperatures between 800 and 950° C, Fig. 3, is interpreted as indicative of blunting of the microcrack by plastic flow at the tip of the crack. At higher temperatures (> 1000° C), the fracture load decreases concomitant with a change in crack growth mechanism (see later).

The first signs of subcritical (slow) crack propagation of the emplaced cracks were observed on the fracture faces in tests made at 1000° C or higher, Fig. 5. The extent of subcritical crack growth prior to catastrophic failure increased as the test temperature increased (cf. Figs. 5a to d). The mode of crack propagation during slow crack growth was revealed clearly by SEM at higher magnifications, Figs. 6a and b, and is entirely intergranular whereas catastrophic failure occurs in a transgranular mode, Figs. 4c and d. The large

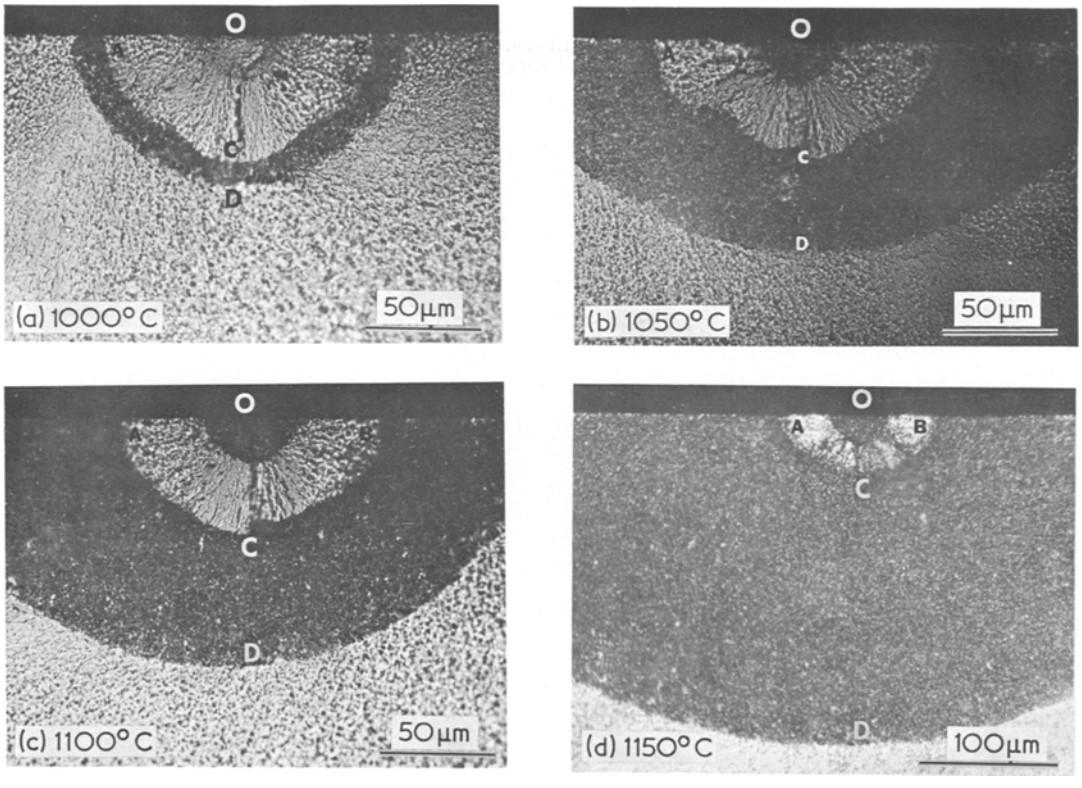

Figure 5 Typical fracture surfaces of LAS specimens precracked with 1000 g load indentation and tested in four-point bending at the marked temperatures. ACB is the original precracked region or initial crack. The dark band surrounding ACB is the slow crack growth region.

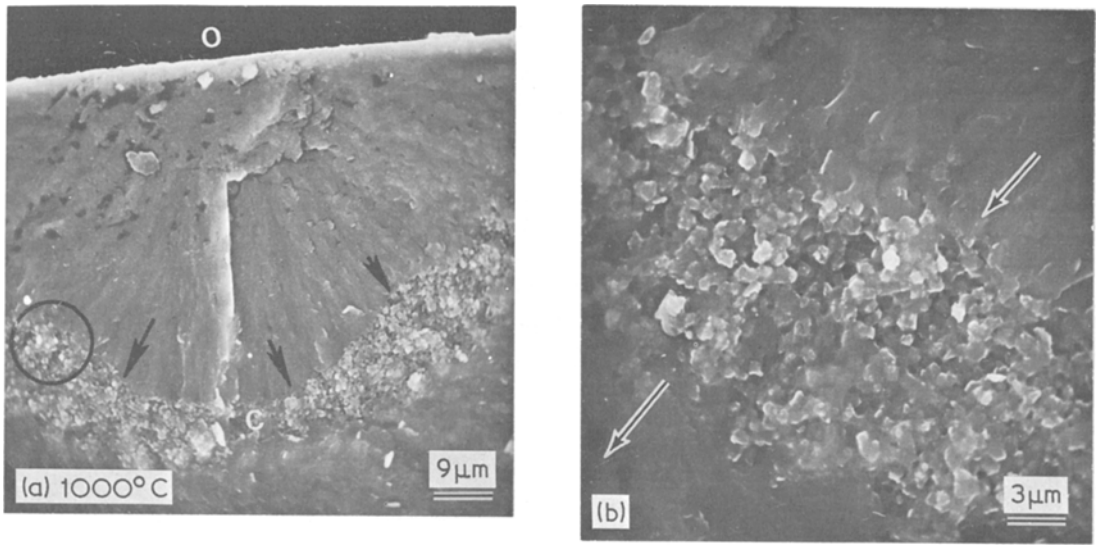

Figure 6 Structure and path of slow crack growth region as revealed in SEM (same specimen as viewed in Fig. 5a). (a) Detailed view of precracked region ACB, arrows indicate the boundary of the initial crack front. (b) The circled area shown in (a) at a higher magnification. Note that the mode of crack propagation in slow crack growth region is intergranular cleavage. Micrograph also shows the transition from the intergranular crack growth to catastrophic cleavage. Arrows indicate the direction of crack propagation.

differences in light scattering from the two types of fracture paths leads to clear demarcation of the slow crack growth region, Fig. 5, under conventional optical light examination. The transition from an intergranular mode of slow crack growth to a transgranular cleavage mode accompanying high speed fracture indicates that a fine balance exists between the alternate crack paths. In high speed fracture, plastic deformation integral to crack growth is minimized due to the very high strain rate in the vicinity of the crack tip, and the crack finds a transgranular path easier than a more deformation-accommodating grain boundary region. During slow crack growth, the crack extends by plastic separation of what appears to behave as a ductile, low viscosity grain boundary glass phase, at stress levels considerably less than that necessary to promote cleavage fracture. When the stress intensity at the tip of the crack has increased sufficiently due to crack lengthening by slow crack growth, a point is reached beyond which fast cleavage fracture is more favourable (the Griffith condition is satisfied) and a transition to high speed catastrophic fracture occurs, Fig. 5. The extent of slow crack growth increases with increasing temperature up to the vicinity of 1150° C, Fig. 5, beyond which the transition to a catastrophic fracture is entirely suppressed and large scale flow occurs in the material.

The influence of initial crack size on the temperature dependence of fracture is shown in Fig. 3. With the smaller crack size (specimens precracked with 500 g indentation load), σ_F is increased relative to specimens precracked with 1000 g indentation load, but the main features of the temperature dependence are the same as discussed above.

3.3. The role of an amorphous phase

Fig. 7 shows data in support of the proposition that a major role in the high temperature fracture behaviour of this material can be assigned to a remnant grain boundary glassy phase. In Fig. 7a, a comparison is provided of the temperature dependence of strength of the crystalline and amorphous states of these otherwise identical materials. While there are distinct differences in the absolute stress level at fracture as well as absolute temperature dependence, the overall material response is similar in form. In both states of consolidation, brittle fracture is observed at temperatures up to that corresponding to the peak in fracture stress. In the crystalline material, the peak appears to correlate with the onset of subcritical crack growth, increasing in extent with increased temperature. In the

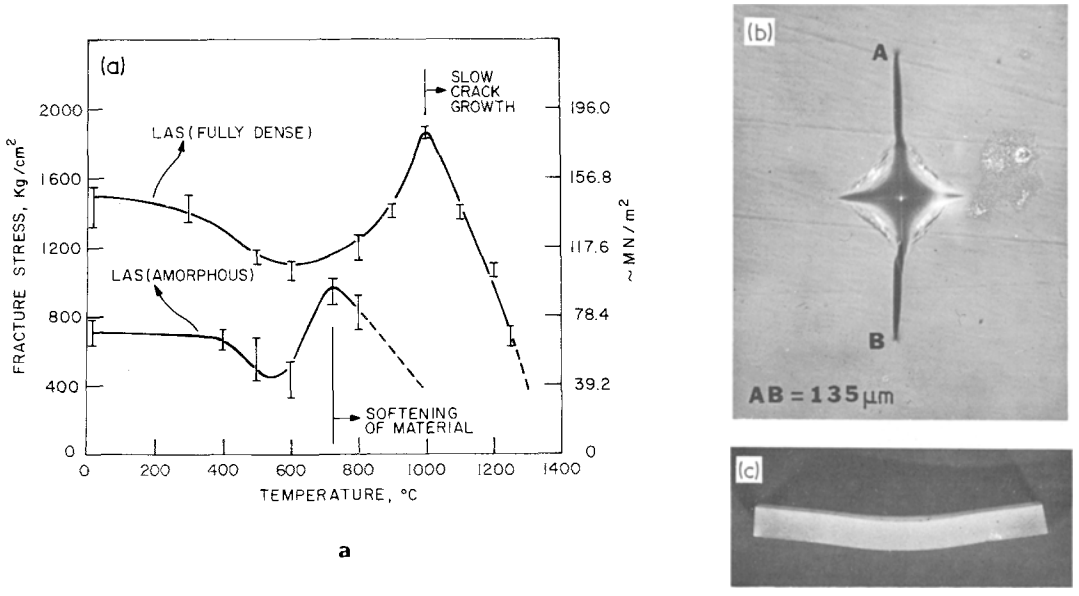

Figure 7 (a) Temperature dependence of the fracture stress for uncracked crystalline and amorphous LAS glass-ceramic specimens. (b) Crack blunting due to softening of glass as observed in a precracked specimen (1000 g load indentation) of LAS (amorphous) material tested at ~ 800° C. (c) Side view of the bent specimen (same as in Fig. 7b).

amorphous material, gross plastic flow occurs at temperatures above the peak in the stress response. At 800° C, this is evidenced by gross plastic flow around emplaced crack (Fig. 7b), a macroscopically apparent permanent set in the material (Fig. 7c), but no accompanying tendency for subcritical crack growth.

While there is an obvious distinction between the amorphous and the crystalline state, the critical factor mechanistically seems to be that of the behaviour of a single phase (amorphous) versus a dual phase aggregate. At the temperature of the peak stress in the amorphous material (~ 720° C), decreasing viscosity with increasing temperature results in increased local crack tip blunting with concomitant increase in fracture strength. The size of the plastic flow region continues to increase until the propagation of blunted cracks and long range plastic yielding (flow) of the viscous media are exactly competitive. At higher temperatures, viscous flow is the dominant stress-accommodating mechanism, flaws being effectively neutralized by plastic deformation, and the ability of the material to support a load decreases along with the viscosity at higher temperatures. The absence of subcritical crack growth in this instance is consistent with the mechanisms at play in this regime. The most important result, however, is that the LAS glass softens significantly in the same temperature range that the crystallized material exhibits an increase in fracture strength consistent with localized plastic strain (i.e., crack blunting). When supplemented by the fractographic evidence, this observation provides the most direct support to date for the mechanisms proposed to account for the temperature dependent fracture behaviour of crystallized glass-ceramics.

The high temperature strengthening response in the crystalline aggregate is due to diminution of the crack tip stress intensity by plastic relaxation in the grain boundary viscous media. Mechanistically, this crack blunting can be envisaged as an incipient crack-branching or slippage along grain boundaries in proportion to the local resolved shear stress within the stress field of the crack tip. This phenomenon occurs in the normally crystalline material within the temperature range of demonstrable plastic flow of the amorphous phase because of the very small relative volume of this material.

3.4. Effects of crack blunting on fracture stress

An attempt was made to confirm the influence of crack tip morphology on the fracture stress and the mode of crack propagation. Specimens were precracked to produce cracks approximately 52 μm in depth (1000 g load indentation) and

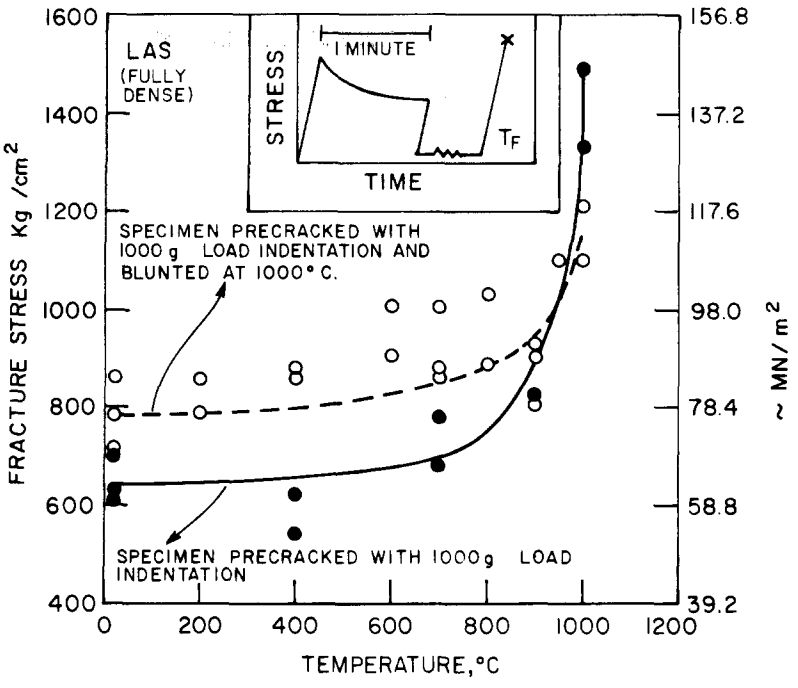

Figure 8 Temperature dependence of the fracture stress for specimens containing sharp and blunted cracks. Specimens in both cases contained cracks of about 52 μm depth. Inset shows schematic representation of plastic blunting at 1000° C in precracked specimens. Specimens were loaded to ~ 0.5 σ_F at 1000° C and the stress was relaxed, unloaded after 1 min and tested at the desired temperature.

subsequently loaded at 1000° C to 0.5 σ_F for the precracked condition, and stress relaxed in the mode shown schematically in Fig. 8 (inset). Stress relaxation (under fixed cross-head position) was continued for 1 min before the specimen was unloaded. This procedure (developed by trial and error) produced an effective plastic blunting of the crack tip without any increase in crack length, as confirmed by an SEM study. The specimens containing cracks blunted in this manner were subsequently tested to failure at the desired temperature.

The variation of σ_F for plastically blunted cracks as a function of temperature is shown in Fig. 8. Compared to specimens containing sharp cracks, it is seen that blunting of the crack tip increased the fracture stress considerably. The fracture stress for blunted and sharp cracks merge together at about 900° C consistent with crack propagation (and the magnitude of σ_F) being controlled by the amount of plastic flow occurring during the test.

3.5. Rate effects

The strain rate sensitivity of the fracture process in LAS was explored at one precrack size and at two temperatures within the regime where subcritical crack growth is a factor. The generic relationship between fracture stress and strain rate (or machine head speed) for specimens containing cracks of about 80 μm depth (indentation load 2000 g) at 950° C and 1100° C is displayed in Fig. 9. As seems typical of this relationship, σ_F initially increases with strain rate, attains a maximum and then drops rapidly to a plateau of strain rate independent behaviour. The variation in fracture surface topography, principally the comparative extent of subcritical crack growth at 1100° C, is illustrated in Fig. 10 for certain of the specimens plotted in Fig. 9. The extent of subcritical crack growth (depth CD in Fig. 10) decreases as the loading rate increases until it disappears in the range of machine head speeds of 0.05 to 0.5 in. min^{-1} and fracture commences catastrophically. The behaviour is similar in kind for each temperature but the curve for the lower temperature (950° C) is shifted down the loading rate scale so that subcritical crack growth decreases and disappears proportionately at a slower strain rate, Fig. 9.

The form of the rate dependence of fracture stress for precracked specimens in the temperature/strain rate regime in which subcritical crack growth is competitive is based on the nature of the plastic response localized at grain boundaries. Two regimes of behaviour are considered. At low temperatures, or high strain rates, the grain boundary film of residual glassy phase is effectively as "hard" as the crystalline grains and the fracture path is transgranular, there being no relative advantage

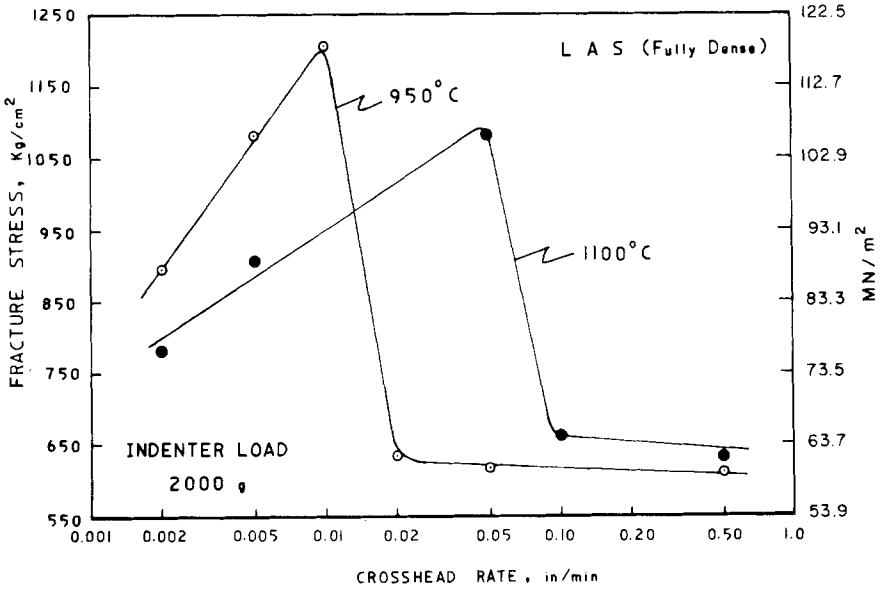

Figure 9 Effect of machine head speed (or strain rate) on temperature and fracture stress for specimens containing a constant crack size (~ 80 μm depth) and tested at two different temperatures, namely 950° C and 1100° C. All specimens were precracked with 2000 g load indentation.

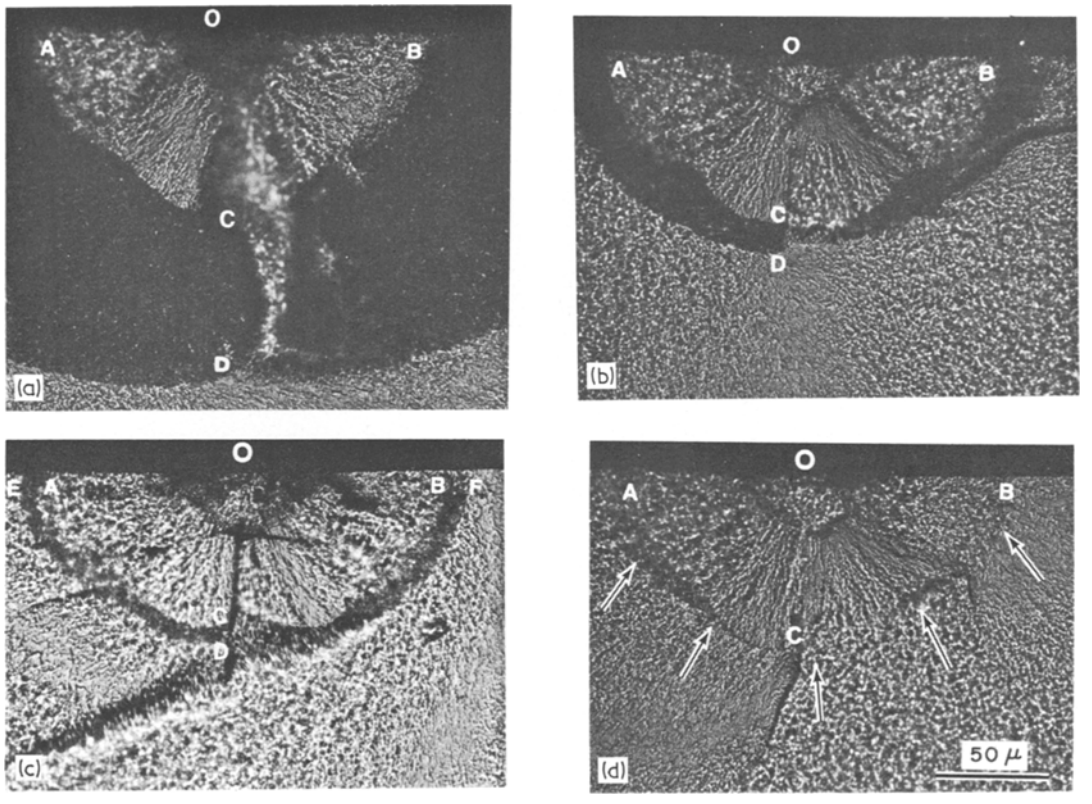

Figure 10 Successive stages in the fractographic appearance of precracked specimens included in Fig. 9 tested at 1100° C as a function of machine head speed. (a) Machine head speed = 0.002 in. min^{-1}; (b) MHS = 0.05 in. min^{-1}; (c) MHS = 0.10 in. min^{-1} and (d) MHS = 0.50 in. min^{-1}.

offered by an intercrystalline route. Toward the higher temperature, or lower strain rate, end of this regime, flaws can be effectively blunted by (bulk) plastic accommodation within the stress field of the crack tip. This leads to the peak in σ_F with increase in temperature after a relatively temperature insensitive low temperature response.

At higher temperature, or equivalently lower strain rates, the viscosity of the grain boundary film decreases sufficiently such that subcritical cracks can grow by intergranular extension. Eventually, the crack enlarges to the point where the material response to the advancing crack tip falls into the high strain rate regime (Griffith criterion) and the subsequent failure is transgranular and rapid (catastrophic).

3.6. Stress rupture response

To demonstrate the phenomenological self consistency of the rate (time) dependent behaviour thus far described, a cursory investigation was made of the extent of subcritical crack growth in precracked specimens (constant initial crack size) loaded to various fractions of the precracked fracture stress, σ_F (at a machine head speed of 0.005 in. min^{-1}) at 1000 and 1100° C. The response observed in the tests at 1000° C are typical and are shown in Fig. 11. A directly analogous set of data is available for the 1100° C tests. Fig. 11a indicates that fracture occurs very rapidly, within 1 to 2 min, when the applied stress is very high. Note the slow crack growth region, CD, has grown rapidly in 1.4 min (cf. Fig. 5a). At a slightly lower stress level, the time to failure increased significantly without a substantial increase in extent of subcritical crack growth, Fig. 11b, indicating a slower rate of slow crack growth. At intermediate stress levels, both the extent of slow crack growth and time to failure increased considerably. At low stress levels, around 0.3 to 0.4 σ_F, the extent of slow crack growth approaches zero and the specimen can sustain the stress for a considerably longer time, Fig. 11c. In the case illustrated, a specimen which did not fail prior to 60 min was unloaded and broken at room temperature to reveal the nature of the slow crack growth region. The original precrack had grown along the surface in response to the maximum tensile fibre stress, from AB to EF as indicated by the slow crack growth region, but did not grow significantly in depth. It appears that there is to be anticipated a critical stress level below which no significant slow crack growth occurs. This parameter could be determined from long term creep tests.

4. Conclusions

(1) At room temperature, fracture stress was found to depend on crack length according to the Griffith criterion. Extrapolation of the data indicate that flaws of the order of 6 to 8 μm are responsible for brittle fracture of virgin (uncracked) specimens.

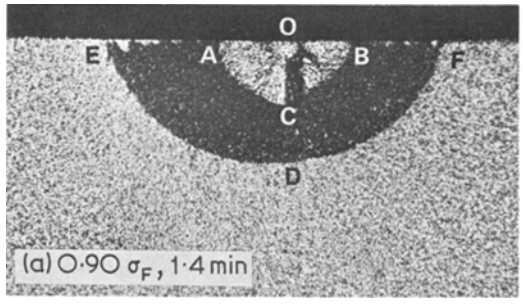

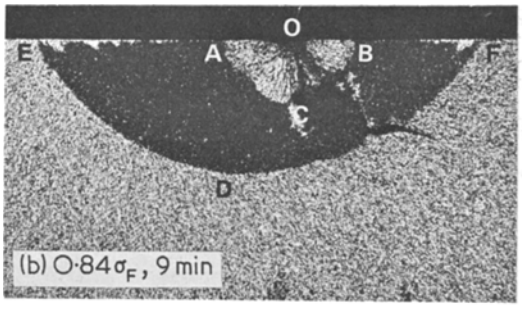

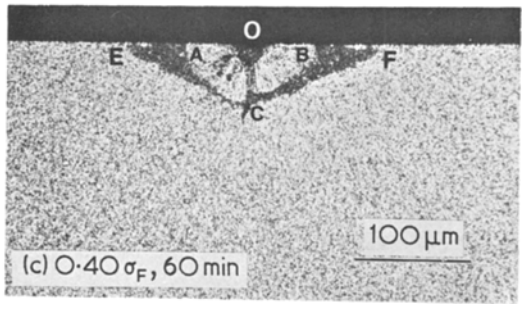

Figure 11 Successive stages in the movement of slow crack growth region of LAS specimens tested at varying stress levels at 1000° C. All specimens were precracked with 1000 g load indentation. (a) Specimen loaded to a stress level of ~ 0.90 σ_F which was kept constant, specimen fractured at the precracked site after 1.4 min. (b) Specimen loaded to a stress level of ~ 0.84 σ_F which was kept constant, and finally failed at the precracked site after 9 min. (c) Specimen loaded to a stress level of ~ 0.4 σ_F which was kept constant for 60 min, and finally unloaded and subsequently broken at room temperature.

(2) In precracked specimens, the fracture stress remained essentially constant from 20 to 800° C, suggesting the absence of crack tip blunting. The subsequent increase in fracture stress from 800° C to about 1000° C appears attributable to blunting of the crack tip due to plastic flow. The mode of crack propagation in this temperature range (20 to 800° C) is entirely *transcrystalline* cleavage.

(3) At temperatures of 1000° C and higher, subcritical crack growth occurs. The extent of slow crack growth increases with increasing temperature and is entirely *intergranular* in nature. Catastrophic crack propagation subsequently occurs when the appropriate combination of crack length and stress level is achieved.

(4) A study of the temperature-dependent fracture behaviour of the material in the uncrystallized (amorphous) state supported the suggested relationship between a remnant grain boundary amorphous phase and the high temperature fracture response.

(5) The extent of subcritical crack growth decreased with increasing loading rate in a manner consistent with the described viscous flow controlled phenomenon.

(6) Accelerated stress-rupture tests at high temperatures suggest a temperature-dependent threshold stress above which subcritical crack growth becomes a factor.

Acknowledgements

The authors are pleased to thank Mr G. Easley for assistance in mechanical testing during the early part of this work and Mr J. D. Janowski for assistance in the SEM. This work was supported in part by the Advanced Research Projects Agency under contract DAAG 46-71-C-0162.

References

1. R. K. GOVILA, *Acta Met.* **20** (1972) 447.
2. P. KENNY, *Powder Met.* **14** (1971) 22.
3. N. INGELSTROM and H. NORDBERG, *Eng. Fract. Mech.* **6** (1974) 597.
4. K. R. KINSMAN, M. YESSIK, P. BEARDMORE and R. K. GOVILA, *Metallography* **8** (1975) 351.
5. K. R. KINSMAN, R. K. GOVILA and P. BEARDMORE, "Deformation of Ceramic Materials", edited by R. C. Bradt and R. E. Tressler (Plenum Press, New York, 1975) p. 465.
6. J. J. PETROVIC, L. A. JACOBSON, P. K. TALTY and A. K. VASUDEVAN, *J. Amer. Ceram. Soc.* **58** (1975) 113.
7. A. A. GRIFFITH, *Phil. Trans. Roy. Soc.* **221** (1920) 163.
8. R. C. SHAH and A. S. KOBAYASHI, "The Surface Crack: Physical Problems and Computational Solutions", edited by J. L. Swedlow (ASME, New York, 1972) p. 79.
9. W. A. FATE, Private Communication, Ford Motor Company, Research Staff (1974).
10. J. J. PETROVIC, R. A. DIRKS, L. A. JACOBSON and M. G. MENDIRATTA, *J. Amer. Ceram. Soc.* **59** (1976) 177.
11. M. V. SWAIN, *J. Mater. Sci.* **11** (1976) 2345.
12. R. K. GOVILA and K. R. KINSMAN, *Amer. Ceram. Soc. Bull.* **57** (1978) 316.

Received 18 October 1977 and accepted 3 February 1978.